

## Supporting Information

### Liquid Metal Gradient Fibers with Reversible Thermal Programmability

Huaizhi Liu, Yumeng Xin, Yang Lou, Yan Peng, Lili Wei, Jiuyang Zhang\*

School of Chemistry and Chemical Engineering, Southeast University, Nanjing, 211189, PR China;  
Jiangsu Hi-Tech Key Laboratory for Biomedical Research, 211189, Nanjing, PR China.

E-mail: [jiuyang@seu.edu.cn](mailto:jiuyang@seu.edu.cn)

Keywords: thermal programmability, liquid metal, gradient, fiber

## **Materials and Methods**

### **1. Materials**

Liquid metal (LM) (Gallium, melting point at 29.13 °C) was purchased from Shenyang Jiabei commercial trading company. The PDMS (Sylgard 184, Dow Corning) was provided by Shanghai Dianjiao consumables center. Heating-shrinkable tube was supplied by Tengfei insulating materials Industrial Co., Ltd. Liquid nitrogen (boiling point 77 K) was purchased from Nanjing Wanqing chemical glassware instrument Co., Ltd.

### **2. Methods**

**Preparation of LM fiber:** LM (Ga) and PDMS precursor (mixed with a curing agent at weight ratio of 10:1) was mechanically stirred (OS20-S) at 100 RPM for 100 seconds with equal volume. Then, the mixture was injected into the heating-shrinkable tube with a syringe and cured at 80 °C for 1 h after being kept at room temperature for 15 h. Finally, the LM fiber was obtained when the heat-shrinkable tube was stripped.

### **Characterization**

**3.1 Morphology characterization:** The microstructure of LM fibers were observed in scanning electron microscope (FEI 3D) and optical microscope (XTL-16B).

**3.2 Mechanical measurement:** The tensile test was performed on a tensile tester (MTS E42) at ambient condition with a speed of 30 mm min<sup>-1</sup>. All the reported values of mechanical properties were the average based on at least three independent measurements for each sample.

**3.3 Differential scanning calorimeter (DSC):** The melting enthalpy of LM fiber was performed on DSC (TA DSC25). LM fiber was heated from room temperature (20 °C) to 43 °C at a rate of 1 °C min<sup>-1</sup> and warm for 20 mins. The melting enthalpy of LM fiber was determined.

Table S1. The effect of PDMS/LM ratio on shape and conductivity of the LM fiber.

LM volume fraction	Below 30%		30%-60%		Over 60%	
Distribution	gradient	non-gradient	gradient	non-gradient	gradient	non-gradient
Shape	no effect	no effect	no effect	no effect	no effect	no effect
Conductivity	insulator	insulator	4000 s/m	insulator	> 4000 s/m	> 2000 s/m

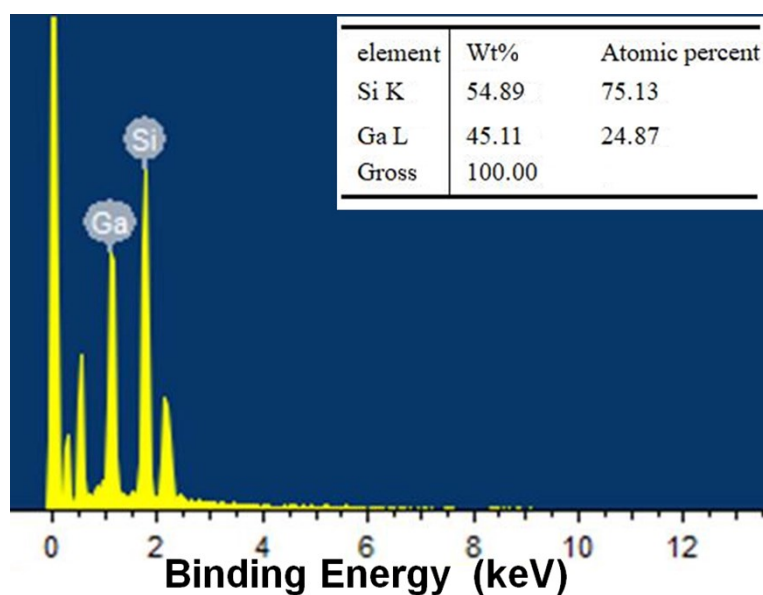
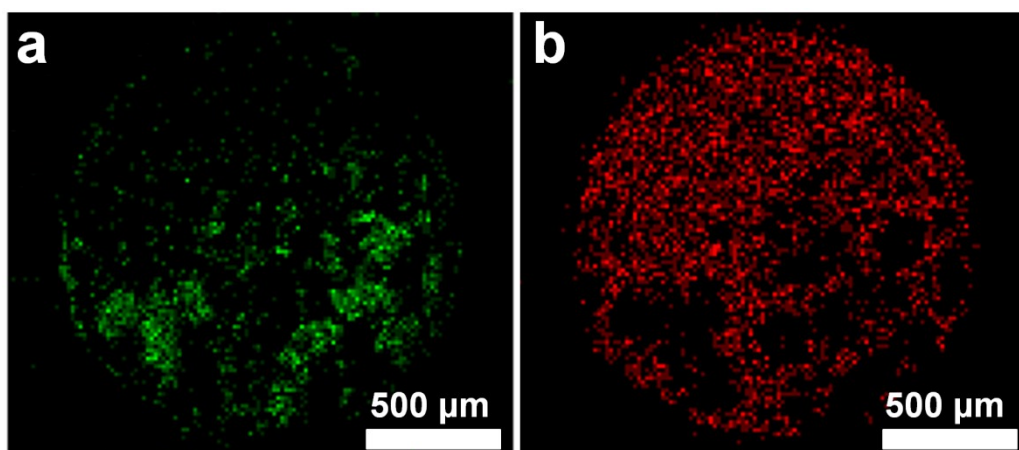
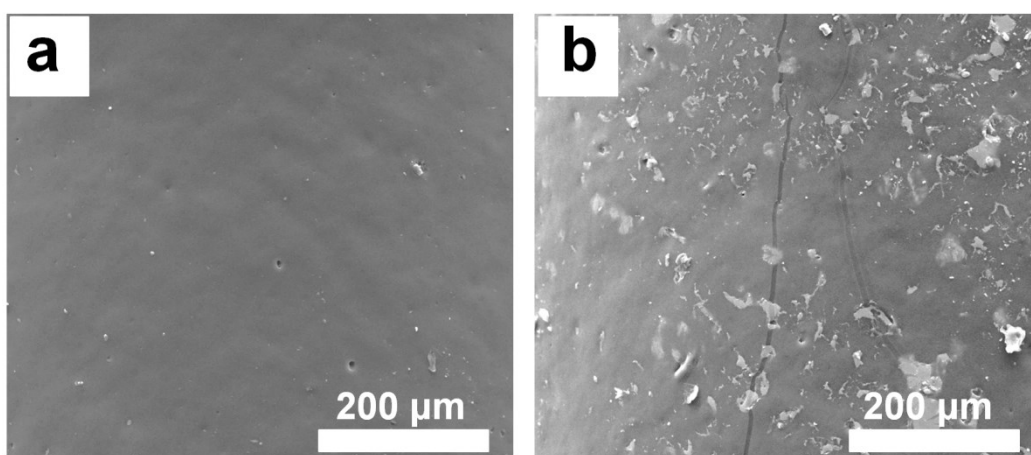


Figure S1. The energy-dispersive X-ray spectroscopy (EDS) spectrum of the LM fiber.



**Figure S2.** The EDS mapping of (a) gallium (Ga, green dot) and (b) silicon (Si, red dot) in the cross-section of LM fiber.



**Figure S3.** (a) The SEM image for the upper surface of LM gradient fiber. (b) The SEM image for the bottom surface of LM gradient fiber.

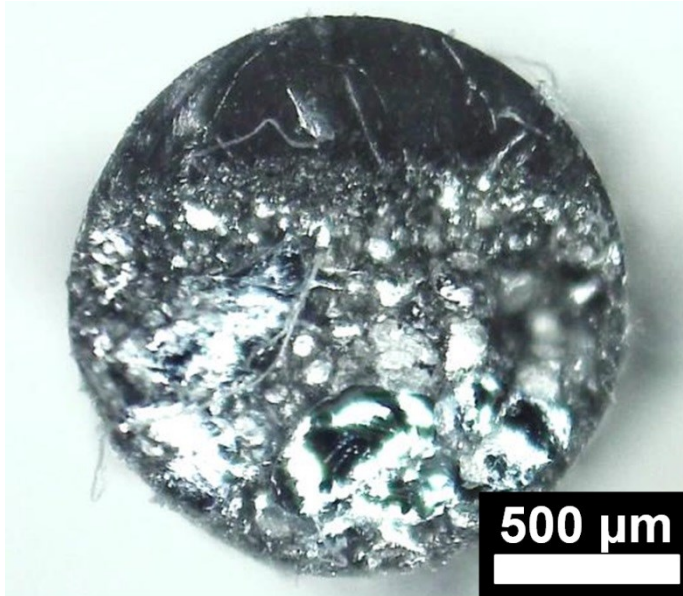


**Figure S4.** The microscopy image in the cross-section of LM gradient fiber (Deposition time before curing: 15 hours). It should be noted that longer and shorter deposition time will lead to non-gradient LM fibers as shown in **Figure S13**.

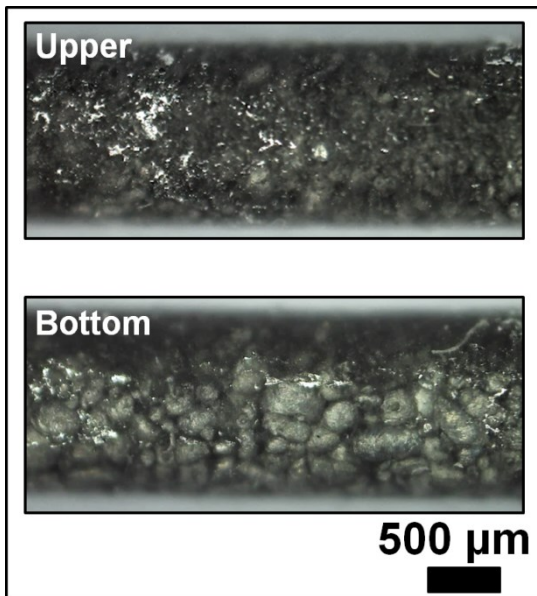


**Figure S5.** The optical microscopy images for the upper and bottom surface of LM fiber.

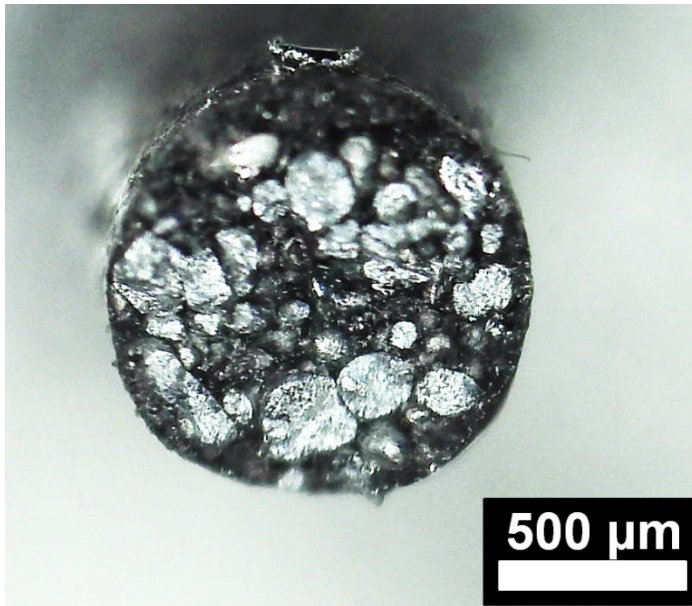


**Figure S6.** The microscope image of the cross-section of finer LM fiber with smaller diameter (near 1.1 mm) was obtained under curing temperature at 90 °C.

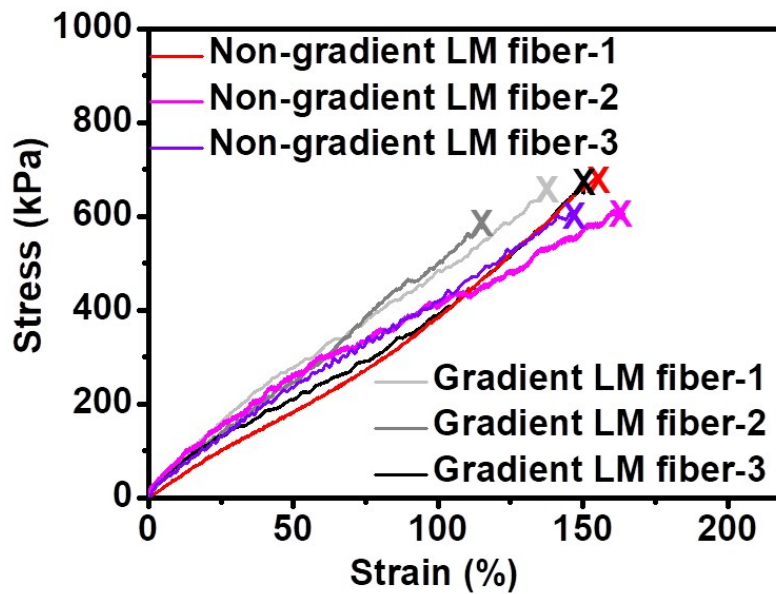


**Figure S7.** Tensile curves of gradient and non-gradient (liquid metal particles are uniformly distributed) LM fibers.

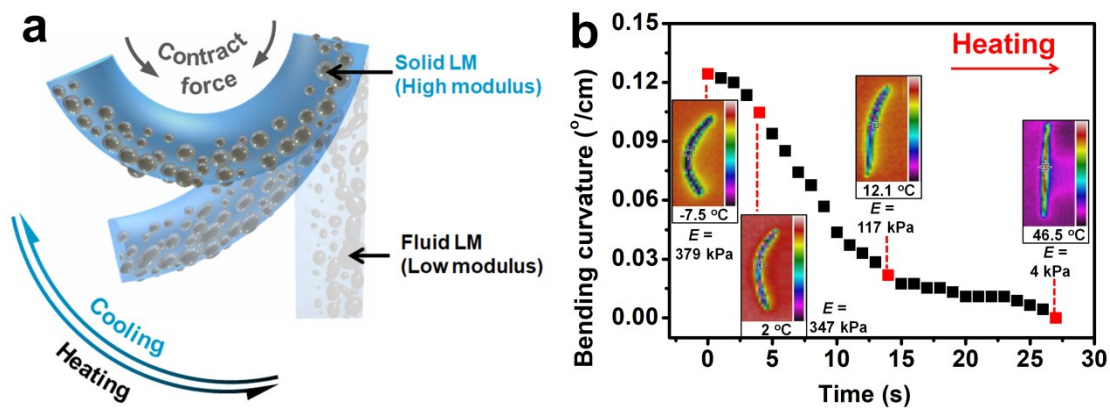


**Figure S8.** (a) The illustration of the modulus and internal contract force for LM fiber under heating-cooling cycles. (b) The moduli change of the LM fiber at different temperature.

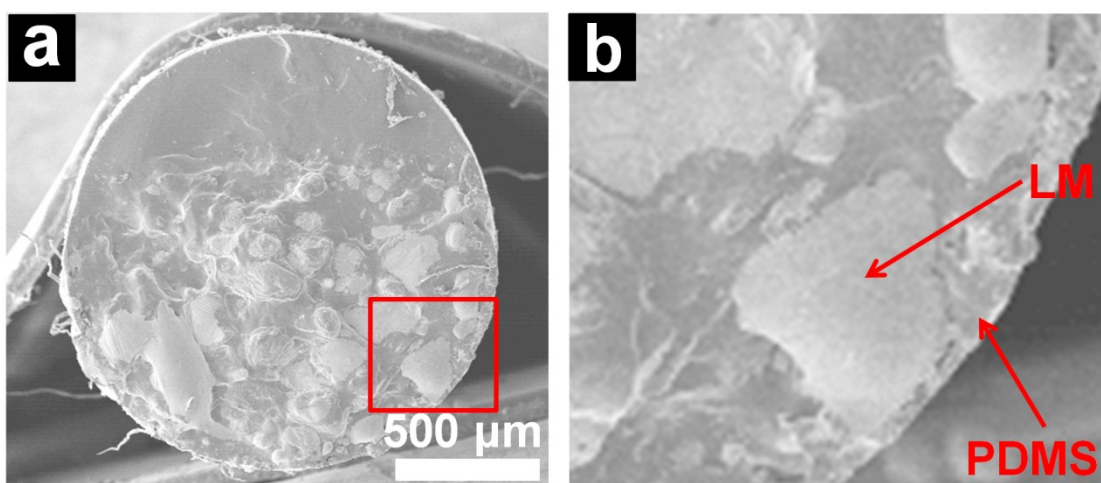


**Figure S9.** (a) Cross-sectional scanning electron microscope (SEM) image for LM gradient fiber. (b) The magnification of SEM image the selected area from **Figure S9a**.

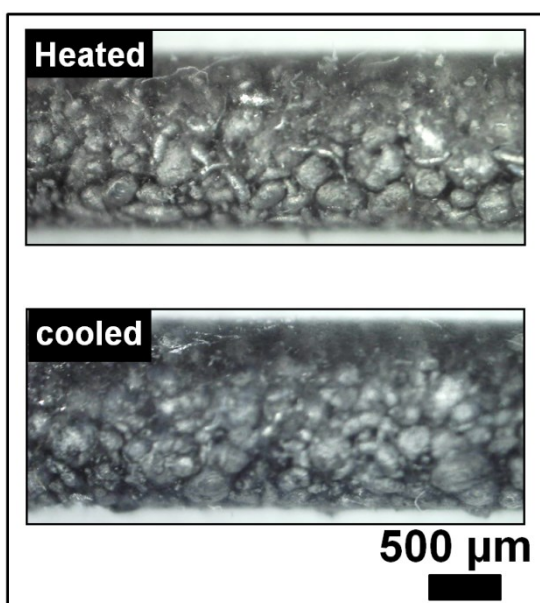


**Figure S10.** The microscopy image for LM gradient fiber under cycle of heating and cooling.

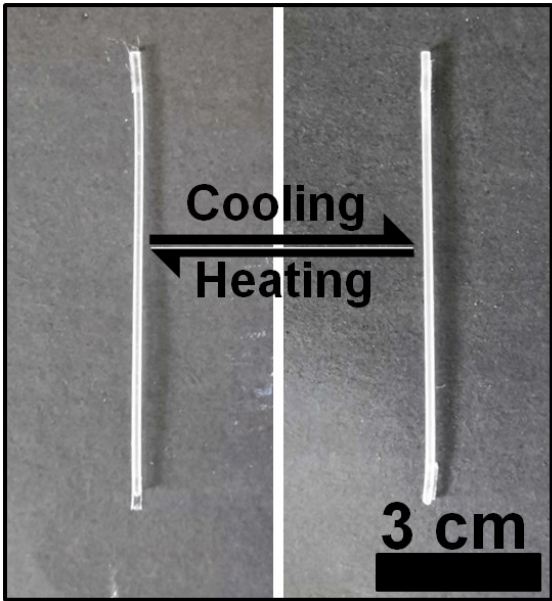


Figure S11. Pure PDMS fiber (8 cm) showed no shape change upon heating (left) and cooling (right).

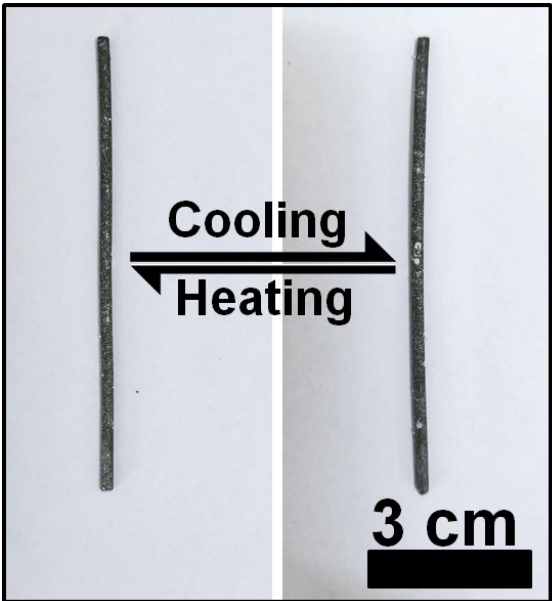
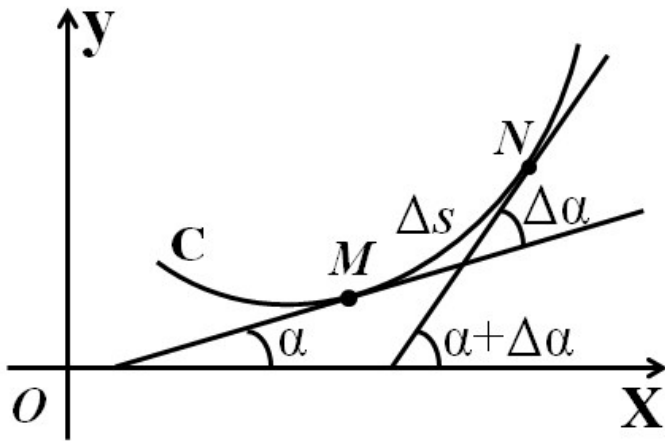
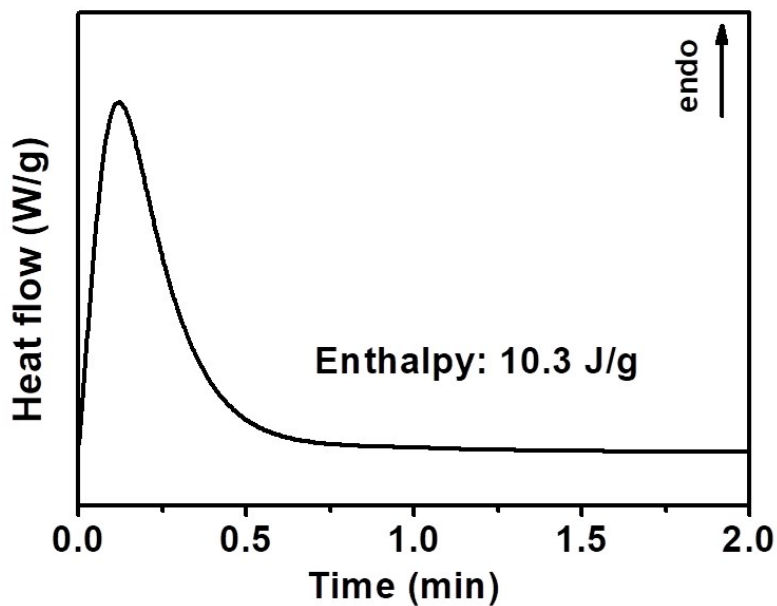


Figure S12. LM fiber without gradient structure (8 cm) showed no shape change upon heating (left) and cooling (right).



**Figure S13.** The illustration diagram of bending curvature calculation. The curve C represents the bent LM fiber, the arc length from point M to point n is  $\Delta s$ , the corner angle of tangent is  $\Delta\alpha$ . The average curvature ( $\bar{K}$ ) of arc  $MN$  can be calculated according to the formula  $\bar{K} = \left| \frac{\Delta\alpha}{\Delta s} \right|$ . ( $\Delta s$ : the arc length from point M to point N;  $\Delta\alpha$ : the corner angle of tangent).



**Figure S14.** The isothermal melting curve (temperature set at 43 °C) for LM fiber via differential scanning calorimeter (DSC) measurement. LM fiber was heated from room temperature (20 °C) to 43 °C at a rate of 1 °C /min and warm for 20 mins. The melting enthalpy of LM fiber was 10.3 J/g.

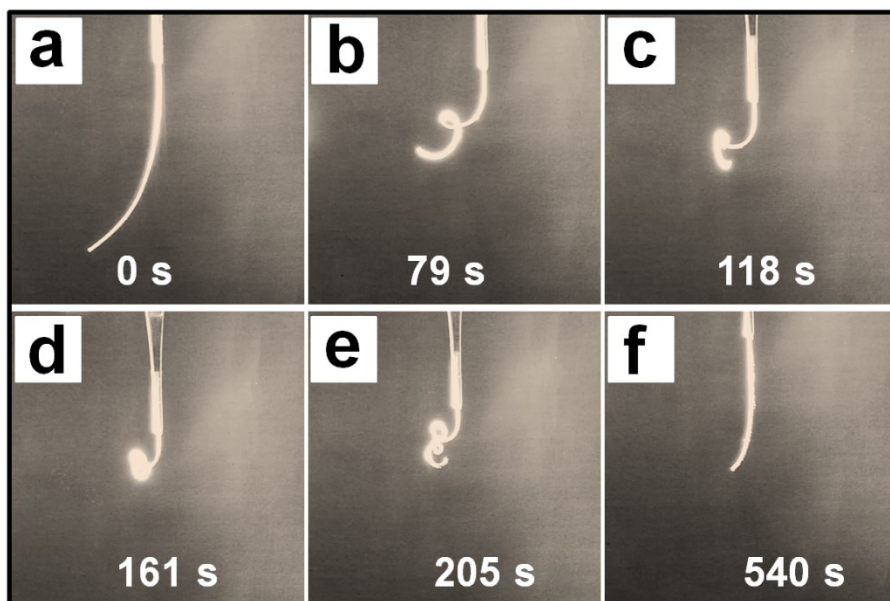


**Figure S15.** The photos to monitor the helical change of the anther cooled and stretched (50% strain) single gradient LM fiber under 75 W heating lamp illuminations. When the stretched (50% strain) and cooled LM fiber was heated, the polymer softened rapidly (the glass transition temperature of PDMS is very low,  $-130\text{ }^{\circ}\text{C}$ ), so PDMS want to go back to the initial length. However, the liquid metal particles are still solid with large moduli. It is difficult to deformation and will prevent fiber returning to its original length. This led to the asymmetric modulus between the liquid metal enriched side and the polymer enriched side of the fiber. The large asymmetric modulus results large bending degree and internal contract force. Only the helical structure can be reduce the difference of shrinkage length. Keeping heating the fiber made liquid metal particles change from solid to liquid, leading to significantly decrease of modulus asymmetry between the enriched side of liquid metal and the enriched side of polymer. As a result, the twisted fibers would recover back to liner ones due to the decrease of internal contract force.

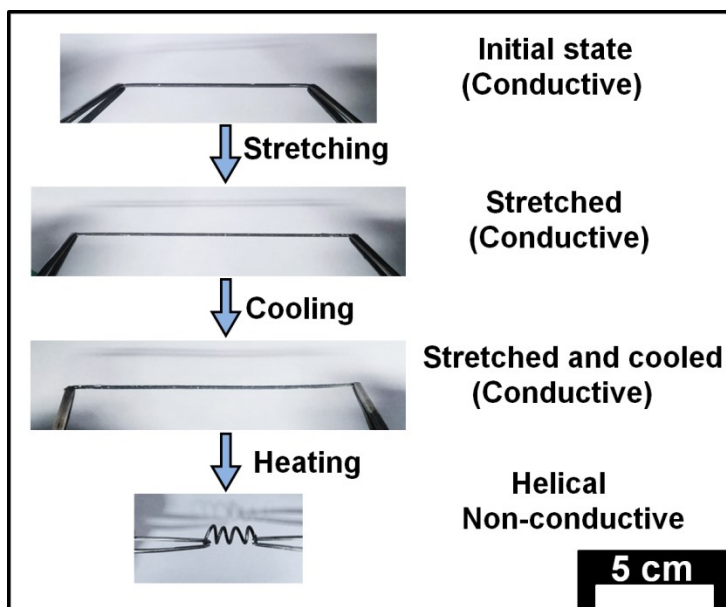


**Figure S16.** The fabrication process of the helical LM fiber. Briefly, the gradient LM fiber (8 cm) was stretched to 50% strain (12 cm), and then cooling down. The helical LM fiber was obtained by heating the stretched (50% strain) and cooled LM fiber.

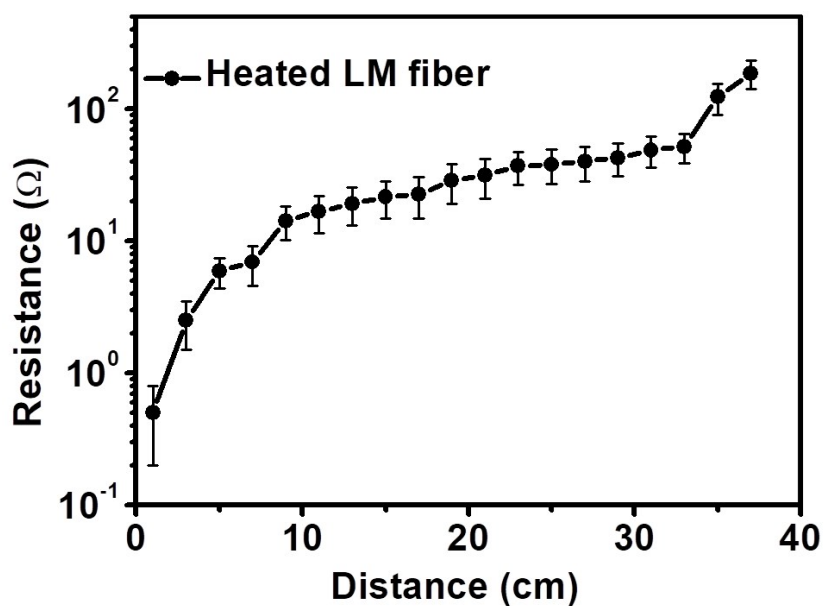


**Figure S17.** The detailed values of the resistance and standard deviation at different distances of the heated LM fiber.

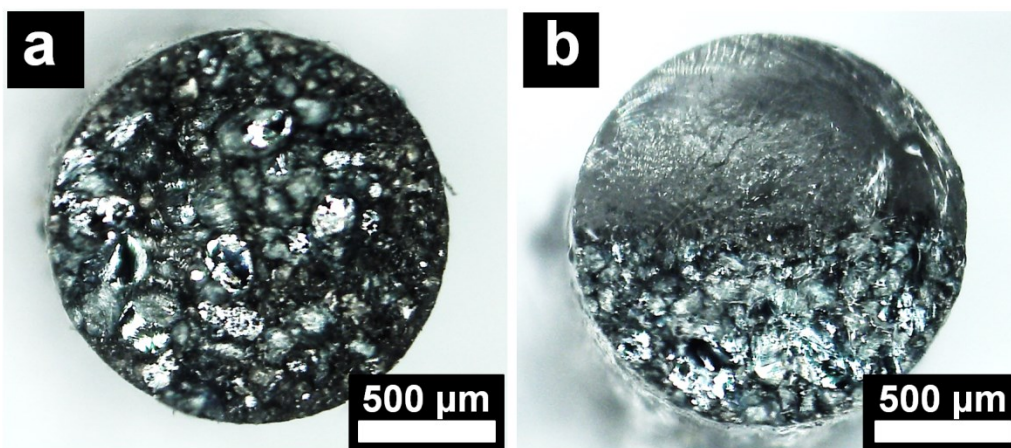


**Figure S18.** The microscopy images in the cross-section of uniformly dispersed LM fiber (deposition time before curing: 0 hour) (a) and fully deposited LM fiber (deposition time before curing: 25 hours) (b).

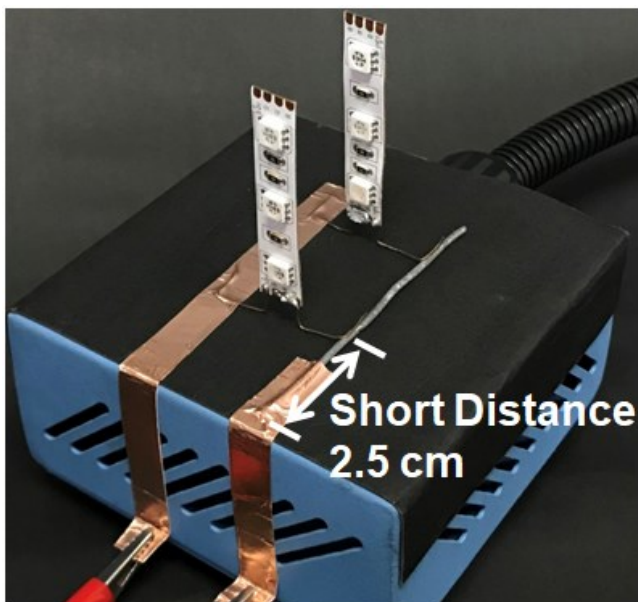


**Figure S19.** A partial enlargement photo of Figure 3d.

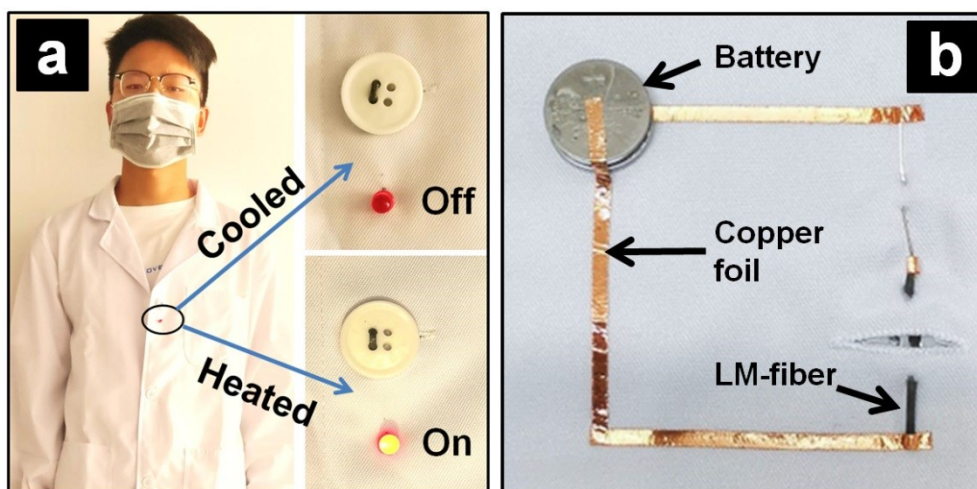


**Figure S20.** The (a) front and (b) back images of gradient LM fiber woven into clothes to tighten the button.

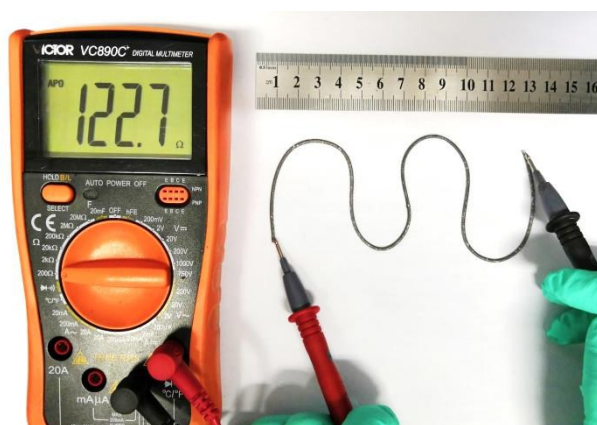


**Figure S21.** The photo of resistance of longer LM gradient fiber with 35 cm.

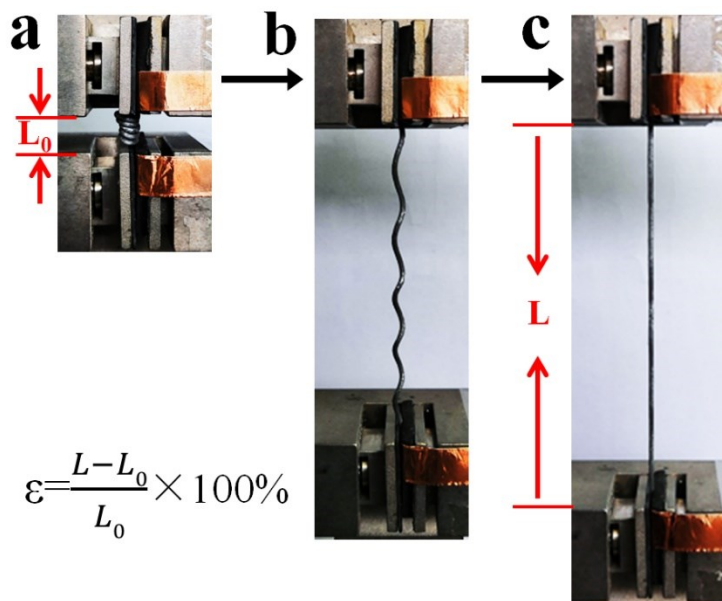


**Figure S22.** The photos of helical LM fiber tensile performance and the calculation formula of tensile stretch ( $\varepsilon$ ). ( $L_0$  and  $L$  are the initial length and final length of LM fiber, respectively)

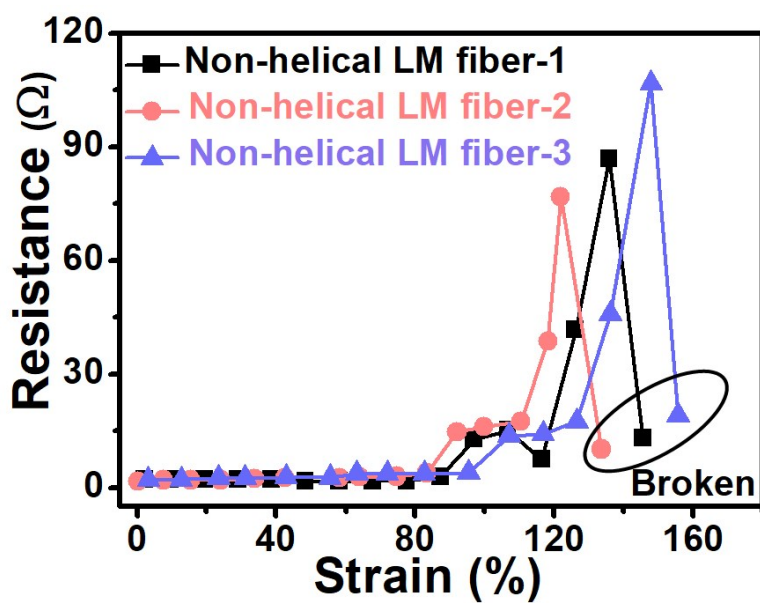


**Figure S23.** The relationship between strain and resistance of gradient LM fibers.

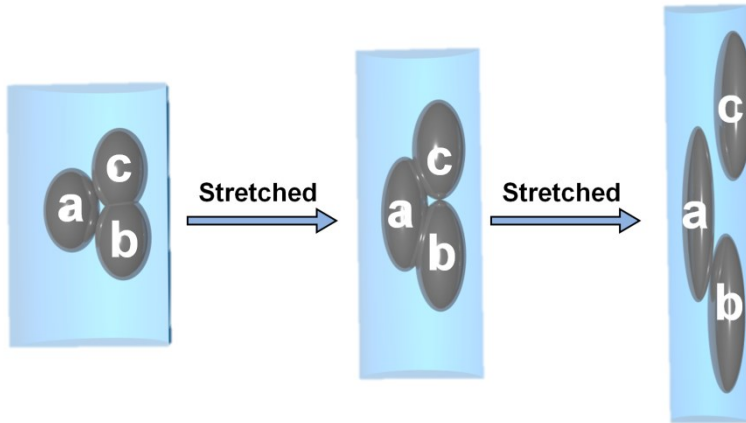


**Figure S24.** Schematic diagram of electrical change of LM fiber during tensile test (**Figure S23**). In the initial state, liquid metal particles “a”, “b”, and “c” are in contact with each other. During the process of stretching, the contact area between particles “b” and “c” decreased gradually, but the particle “a” contacted with “b” and “c” closely due to the increased length in tensile direction but decreased diameter of the fiber under tensile force. This may be the reason for the resistance of the LM fiber keeps constant up to 80%. When the fiber was kept being stretched, the particle of “c” was separated with “a” and “b”, and the contact area between “a” and “b” would reduce, resulting in increased resistance. As for the phenomenon that the resistance of the fiber has a sharply drop near breaking, we suspected that near breaking, the liquid metal particles are squeezed out at the breaking position of the fiber to form a transient conductive pathway at the breaking point.

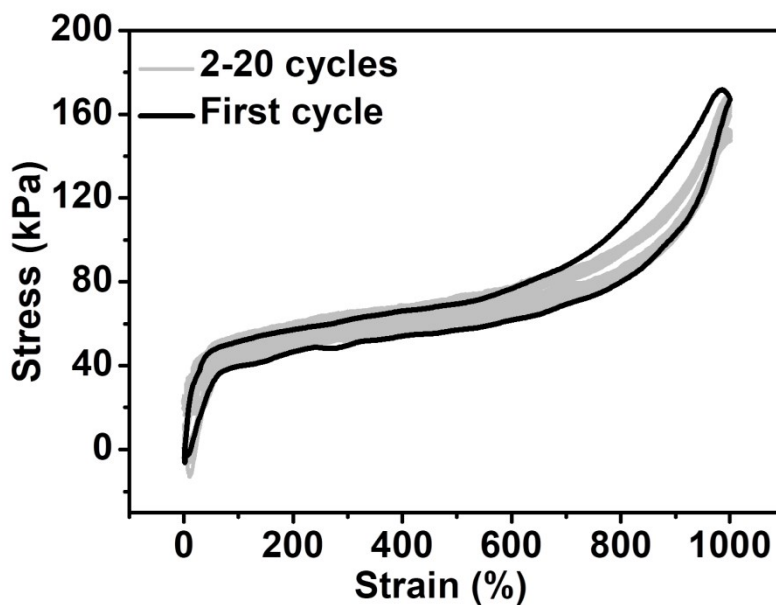


**Figure S25.** The tensile curves of the helical LM fiber under 20 loading-unloading cycles.

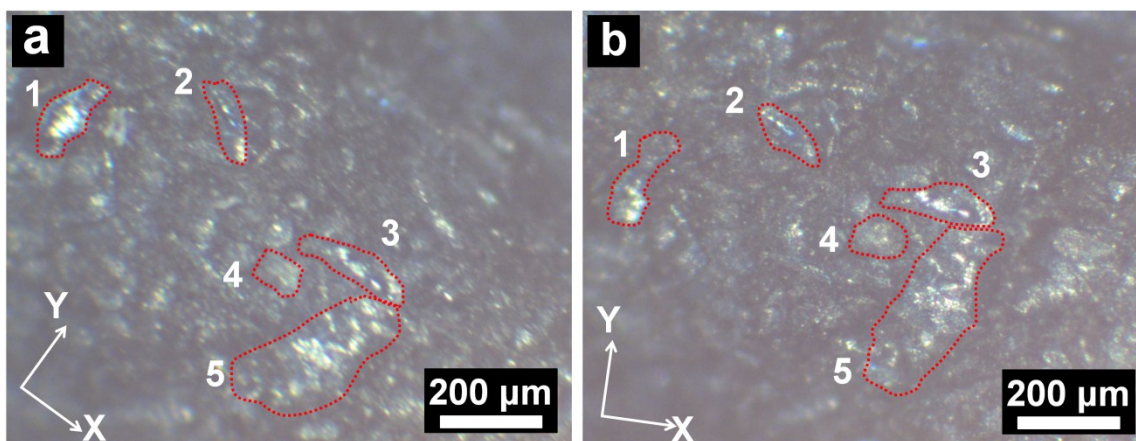


**Figure S26.** The representative optical microscopy images for the LM particles size distribution of the helical LM fiber before and after being stretched (strain about 600%).

**Table S2.** The size change of LM particles for helical LM fiber in X-axis direction under stretching in X direction.

Size in X-direction (Helical)	Size in X-direction (Stretched)	Shrinkage%
185	173	6.486486486
270	257	4.814814815
140	131	6.428571429
132	130	1.515151515
117	109	6.837606838
131	125	4.580152672
162	149	8.024691358
52	50	3.846153846
146	142	2.739726027
35	31	11.42857143
144	132	8.333333333
177	162	8.474576271
75	69	8
115	108	6.086956522
190	177	6.842105263
241	229	4.979253112
69	62	10.14492754
97	92	5.154639175
258	247	4.263565891
30	28	6.666666667
25	24	4
156	151	3.205128205
186	177	4.838709677
107	101	5.607476636
88	82	6.818181818
79	72	8.860759494

---

92	90	2.173913043
158	150	5.063291139
82	78	4.87804878
58	55	5.172413793
76	71	6.578947368
42	36	14.28571429
160	145	9.375
33	30	9.090909091
120	111	7.5
159	150	5.660377358
132	125	5.303030303
148	140	5.405405405
81	71	12.34567901
48	42	12.5
62	56	9.677419355
30	26	13.33333333
118	84	28.81355932
117	75	35.8974359
203	182	10.34482759
150	130	13.33333333
100	90	10
62.5	50	20
275	250	9.090909091
280	230	17.85714286
80	60	25
75	70	6.666666667
210	190	9.523809524
18	15	16.66666667
62	49	20.96774194
53	50	5.660377358
110	102	7.272727273
96	91	5.208333333
77	69	10.38961039
44	40	9.090909091
72	66	8.333333333
93	84	9.677419355
42	39	7.142857143
88	79	10.22727273
71	65	8.450704225
97	89	8.24742268
32	30	6.25
142	131	7.746478873
150	141	6
99	87	12.12121212

---

160	151	5.625
200	183	8.5
77	69	10.38961039
75	69	8
88	81	7.954545455
97	89	8.24742268
74	69	6.756756757
77	65	15.58441558
73	68	6.849315068
144	134	6.944444444
104	92	11.53846154
166	151	9.036144578
88	84	4.545454545
107	97	9.345794393
225	210	6.666666667
103	94	8.737864078
52	49	5.769230769
91	85	6.593406593
117	103	11.96581197
107	101	5.607476636
125	118	5.6
165	153	7.272727273
238	208	12.60504202
185	173	6.486486486

**Table S3.** The size change of LM particles for helical LM fiber in Y-axis direction under stretching in X direction.

Size in Y-direction (Helical)	Size in Y-direction (Stretched)	Expansion%
36	44	22.22222
21	29	38.09524
40	49	22.5
185	191	3.243243
40	67	67.5
77	83	7.792208
61	68	11.47541
30	31	3.333333
42	48	14.28571
180	194	7.777778
46	54	17.3913
72	79	9.722222
32	35	9.375
33	35	6.060606
33	45	36.36364

---

25	33	32
190	205	7.894737
42	45	7.142857
41	49	19.5122
77	83	7.792208
272	289	6.25
58	62	6.896552
42	46	9.52381
85	93	9.411765
117	125	6.837607
135	147	8.888889
101	105	3.960396
47	53	12.76596
68	75	10.29412
140	149	6.428571
111	120	8.108108
210	225	7.142857
65	77	18.46154
69	77	11.5942
94	103	9.574468
40	44	10
91	96	5.494505
102	110	7.843137
131	142	8.396947
87	92	5.747126
151	160	5.960265
183	205	12.02186
101	104	2.970297
59	64	8.474576
59	83	40.67797
110	125	13.63636
60	63	5
50	55	10
25	30	20
70	85	21.42857
180	200	11.11111
90	101	12.22222
42	48	14.28571
60	63	5
73	81	10.9589
85	96	12.94118
140	148	5.714286
125	132	5.6
130	139	6.923077

---

---

150	159	6
118	125	5.932203
121	130	7.438017
180	195	8.333333
143	156	9.090909
156	163	4.487179
60	67	11.66667
85	91	7.058824
71	81	14.08451
30	39	30
42	48	14.28571
56	62	10.71429
25	30	20
88	97	10.22727
30	33	10
142	153	7.746479
107	112	4.672897
102	111	8.823529
145	160	10.34483
143	155	8.391608
82	97	18.29268
76	84	10.52632
51	58	13.72549
121	131	8.264463
46	54	17.3913
36	42	16.66667
111	120	8.108108
170	185	8.823529
132	143	8.333333
41	48	17.07317
76	85	11.84211
42	46	9.52381
46	54	17.3913
110	130	18.18182

---

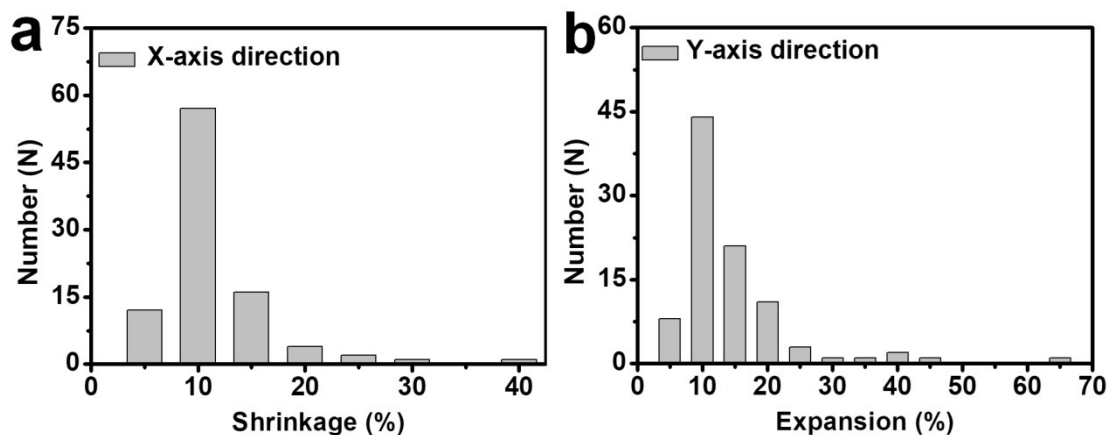


**Figure S27.** Statistical histogram of the size change of LM particles for helical LM fiber from **Tables S2** (a) and **S3** (b). The fiber was stretched in x direction. The particles were shrunk in x direction while expands in y direction.

#### Supporting videos:

**Video S1.** The video S1 was the bending performance of LM fiber under cooling-heating condition.

The bent and cooled LM fiber was heated with a heating lamp to recover back to straight state.

**Video S2.** The video S2 was the helix transformation of LM fiber. Initial strain (50%) was applied on LM fiber during the cooling. Then the stretched and cooled LM fiber was heated by heating lamp (75 W) to show the helical change.

**Video S3.** The video S3 was the test of LM fiber to control the light on and off. The cooled LM fiber (5 cm) was connecting two LED lights. Initially, only one LED was lighted. When the heating device was turn on, the other LED was lighted.

**Video S4.** The video S4 was the process of robot car from static to motional under the illumination of heating light. The wire of the robot was replaced by a cooled LM fiber (5 cm). After heating by the light, the robot car was moved in short time.

**Video S5.** The video S5 was the transition from insulator to conductor of LM fiber upon stretching. Both ends of the copper wire was connected by the helical LM fiber, the LED light was on when the LM fiber was stretched.